

# Results of a 2000-Hour Wear Test of the NEXIS Ion Engine

IEPC-2005-281

*Presented at the 29<sup>th</sup> International Electric Propulsion Conference, Princeton University,  
October 31 – November 4, 2005*

John Steven Snyder,<sup>\*</sup> Dan M. Goebel,<sup>†</sup> James E. Polk,<sup>†</sup> Analyn C. Schneider,<sup>\*</sup> and Anita Sengupta<sup>\*</sup>  
*Jet Propulsion Laboratory, California Institute of Technology, Pasadena, CA, 91109*

The Nuclear Electric Xenon Ion System (NEXIS) ion thruster was developed for potential outer planet robotic missions under NASA's Prometheus program. This engine was designed to operate at power levels ranging from 16 to over 20 kWe at specific impulses of 6000 to 7500 s for burn times of up to 10 years, satisfying the requirements of nuclear electric propulsion systems such as that on the proposed Prometheus 1 mission to explore the icy moons of Jupiter. State-of-the-art performance and life assessment tools were used to design the thruster. Following the successful performance validation of a Laboratory Model thruster, Development Model hardware was fabricated and subjected to vibration and wear testing. The results of a 2000-hour wear test are reported herein. Thruster performance achieved the target requirements and was steady for the duration of the test. Ion optics performance was similarly stable. Discharge loss increases of 6 eV/ion were observed in the first 500 hours of the test and were attributed to primary electron energy decreases due to cathode insert conditioning. Relatively high recycle rates were observed and were identified to be high-voltage-to-ground arcs in the back of the thruster caused by wire insulation outgassing and electron penetration through the plasma screen. Field emission of electrons between the accelerator and screen grids was observed and attributed to evolution of field emitter sites at accelerator grid aperture edges caused by ion bombardment. Preliminary modeling and analysis indicates that the NEXIS engine can meet mission performance requirements over the required lifetime. Finally, successful validation of the NEXIS design methodology, design tools, and technologies with the results of the wear test and companion performance and vibration tests presents significant applicability of the NEXIS development effort to missions of near-term as well as long-term interest for NASA.

## I. Introduction

Interest in science objectives at the outer solar system, specifically at the moons of Jupiter, has recently spurred the development of high-power electric propulsion systems. Such missions require high-power, high-Isp thruster operation and long life that represent major increases over the capabilities of state-of-the-art ion engines. For example, preliminary requirements for the proposed Jupiter Icy Moons Orbiter mission are for thrusters that operate at specific impulses of 6000-9000 sec and powers of 20-50 kW with throughputs greater than 2000 kg.<sup>1</sup> As a part of the Nuclear Electric Xenon Ion System (NEXIS) project,<sup>2</sup> a JPL-led team has developed a thruster designed to meet the life and performance goals and has demonstrated the required performance in laboratory tests.<sup>3</sup> Two development-model NEXIS thrusters have been fabricated and have been demonstrated to meet the performance objectives<sup>4</sup> and to survive launch loads.<sup>9</sup>

The NEXIS thruster was originally proposed in response to a recent NASA Research Announcement (NRA) which solicited proposals to identify and develop thruster technologies that enable nuclear electric propulsion missions to the outer planets. Under this NRA, the JPL-led team proposed and was awarded funding to develop a thruster with a single-operating-point design at a nominal power of 22 kW, providing a specific impulse of 7500 sec

---

<sup>\*</sup> Member of the Technical Staff, Advanced Propulsion Technology Group, Member AIAA.

<sup>†</sup> Section Staff, Propulsion and Materials Engineering Section, Member AIAA.

at 78% total efficiency and a throughput of 2000 kg. Later, the NASA Prometheus program was established to develop nuclear power and electric propulsion for exploration. The NEXIS project became part of Prometheus and, along with continued technology development, supported mission planning for the proposed Jupiter Icy Moons Orbiter mission. Performance requirements for NEXIS were transitioned from the original NRA requirements to those for the Prometheus program.

The NEXIS Laboratory Model (LM) thruster was designed to meet the NRA requirements as well as the additional objectives of operation at  $I_{sp}$ 's in the range of 6500 to 8500 sec with high efficiencies at powers of 15 to 25 kW.<sup>3</sup> The LM thruster design is based on the heritage ring-cusp design successfully used in the NSTAR<sup>5</sup> and XIPS<sup>6</sup> ion thrusters, wherein a hollow-cathode discharge is produced in a cylindrical-conical discharge chamber with magnetic multipole confinement of charged particles, and the ion beam is extracted with an electrode set to produce thrust at high  $I_{sp}$ . The NEXIS design departs from NSTAR and XIPS with the use of a graphite keeper and carbon-carbon grids to provide the required life. The discharge chamber and magnetic field circuit were designed with physics-based models, validated by test, to provide a high efficiency and flat beam profile. The NEXIS LM thruster design met all of its performance goals for the NRA and the JIMO mission without re-design using experimental iteration. It achieved over 78% efficiency at 7500 sec and 25 kW of power with a beam flatness parameter of 0.82, validating the design tools and methodology and providing useful performance data for mission planners.<sup>3</sup>

Following the success of the LM thruster design and test, the design was transitioned to Development Model (DM) hardware, i.e. hardware that is designed to pass dynamic and thermal environmental testing while meeting all performance and lifetime criteria. Since the LM hardware met all performance objectives, there were no changes to the electromagnetic or fluid designs. In order to meet dynamic requirements, the flat carbon-carbon ion optics were replaced with a dished set of optics specifically designed for vibration tolerance. Performance-based design criteria were handed off to industry, where the mechanical design of the NEXIS DM thruster was completed. Two DM thrusters were fabricated; DM1a was used for performance and wear testing,<sup>4</sup> and DM1b was used for vibration testing.<sup>9</sup> The DM1b thruster was also subjected to post-vibration functional testing and demonstrated performance similar to or exceeding DM1a.

The focus of this paper is the results of a 2000-hour wear test of the NEXIS DM11 ion engine. The test had three main objectives: (1) to establish test conditions that provide reasonable assurance of obtaining representative results for final flight conditions and hardware; (2) to characterize the operation of the thruster over the duration of the test, including any performance degradation; and (3) to characterize the wear of the engine and its components, including the wear rates of known wear modes and identification of unanticipated wear phenomena. An ancillary goal is to demonstrate adequate thruster design maturity for the project to progress to the next development step toward flight hardware.

An overview of the NEXIS project, including a discussion of the design and fabrication of the DM, is provided in Ref. 2. Discussion of the carbon-carbon ion optics may be found in Ref. 7. Structural design and analysis of the engine is discussed in Ref. 8. Comparison of performance data from the DM1a engine to the models used in engine design are provided in Ref. 4. Results from the vibration test of the DM1b engine are discussed in Ref. 9.

## II. Test Setup

### A. Test Article

The NEXIS Development Model 1a (DM1a), shown in Fig. 1, served as the test article for the wear test. In brief, the thruster consisted of a 65-cm-dia cylindrical-conical discharge chamber with six magnet rings forming the ring-cusp magnetic field which closed the 60 G contour along the entire anode surface. A plasma-spray coating of the same stainless-steel material as the chamber construction was applied to the interior of the chamber to provide for flake retention. The physical and electromagnetic designs of the chamber were accomplished using state-of-the-art ion thruster design tools developed at JPL. The discharge

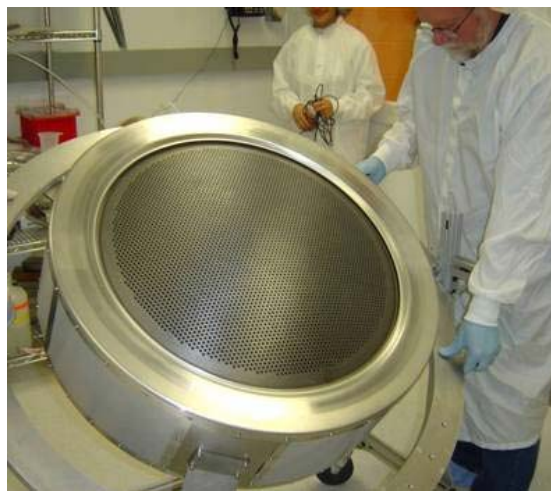


**Figure 1. NEXIS DM1a Ion Engine.**

chamber and propellant feed lines, including isolators, were welded as assemblies. A conventional laboratory model cathode with a graphite keeper was used for the wear test. The DM thrusters were fabricated using standard JPL flight hardware processes and documentation, yielding a complete set of Assembly Inspection Data Sheets (AIDS).

The NEXIS carbon-carbon ion optics represent the culmination of development efforts led by JPL over the last several years [REF JPC05 NEXIS grids]. The optics were designed for engine performance and life based on JPL's state-of-the-art 2D and 3D plasma simulation codes, and for structural robustness based on design tools developed and validated under the C BIO project [REF]. Grid thicknesses and dish depth were chosen as compromises between performance objectives and structural requirements. The structural design of the optics was validated in the DM1b thruster vibration test [REF]. An intragrid electric field strength of 2.2 kV/mm was chosen for the optics design based on a detailed study of the voltage standoff capability and surface sensitivity to arc damage [REF Dan HV arc]. The active beam diameter of the NEXIS ion engine is 57 cm, slightly smaller than the discharge chamber radius to provide a good plasma profile and small peak-to-edge ion current density to the grids. Bipod flexures were chosen as the interface between the carbon-carbon ion optics and the metal discharge chamber to absorb the difference in thermal expansion of the two assemblies.

The thruster ground screen was originally designed to be similar to the design used in NSTAR-class thrusters, where the majority of the screen is a fine mesh material. Preliminary performance testing before the wear test, however, identified the significant mesh area in back of the thruster as a penetration point for plasma electrons which could be accelerated to high energies and create plasma discharges within the rear ground-screen-to-thruster cavity. In order to prevent such discharges during the wear test the majority of the plasma screen was covered with solid metal masking.

Finally, neutralizer requirements for the NEXIS ion engine were similar to that of the NEXT ion thruster developed by the NASA Glenn Research Center (GRC) [REF], so this design was baselined for the NEXIS thruster. A brazed NEXT neutralizer assembly was provided by GRC for the DM1a wear test.

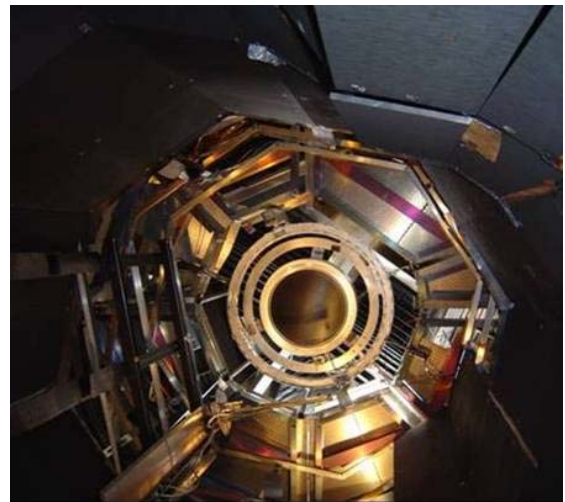


**Figure 2. NEXIS DM1a Ion Engine in Wear Test Facility.**

## **B. Test Facility and Support Equipment**

NEXIS DM thruster testing was performed in a JPL facility converted from use for spacecraft thermal-vacuum testing into an ion thruster test facility. The vacuum tank is 4 m in diameter and 12 m long, with its cylindrical axis oriented vertically and the ~2-3m of the tank extending above the roof of the enclosing building. The walls and bottom end of the facility are lined with water-cooled shrouds for management of the thermal load caused by thruster operation at 20 kW. Additionally, the chamber is lined with graphite panels to reduce metallic backscatter onto the thruster. The shrouds and panel reduce the effective size of the chamber to 2.4-m dia. with the thruster located 7.6-m from the water-cooled, graphite chevron beam dump. A photograph of the DM1a thruster in the test facility is shown in Fig. 2. The facility has a total of ten cryopumps; six nude CVI pumps at the tank ceiling level above the thruster, two low-pumping-speed cryotubs mounted to wall originally used for spacecraft thermal vacuum testing, and four cryosails mounted at the bottom of the chamber behind the chevroned beam dump. The total pumping speed on xenon is initially 250 kL/sec and falls to 200 kL/sec as the chamber reaches thermal equilibrium, which typically takes about 24 hours of thruster operation at 20 kW. The facility backscatter rate was measured with a water-cooled quartz crystal micrograph mounted near the thruster to be 7.5  $\mu\text{m}/\text{hr}$  during performance testing prior to initiation of the wear test.

Power supplies for thruster operation are located on the upper level of the test facility building, close to the engine location. A Diversified Technologies, Inc., 8-kW, 4.5-A supply is used for the beam supply. This power supply was specially designed with a fast-acting switch that opens the load circuit within about 10  $\mu\text{s}$ , thereby limiting the charge transfer in a high-voltage arc to 1 mC. This charge transfer limit was derived from testing of the carbon-carbon optics materials and limits surface roughening which can cause reduced voltage standoff [REF Dan 2005 HV Breakdown JPC]. The accelerator grid power supply is a standard Glassman 1.5-kV, 2-A supply which was factory-modified to reduce the stored energy. The thruster discharge is run with a 55 V, 55 A Sorenson. A 25-

V relayed supply was incorporated into the thruster circuit for performing screen grid ion transparency measurements. NIST-traceable calibrations were performed for all voltage- and current-measuring shunt resistors.

The engine recycle circuit was developed using a dedicated National Instruments PXI chassis and a Labview-based Real Time software module. The recycle hardware detects a screen undervoltage condition, produced when the beam supply fast-acting switch opens, and initiates a recycle. A pulse counter is used to record the recycle rate. All recycle parameters are software programmable for flexible engine test conditions. The data acquisition and control system (DACS) was derived from that successfully for the NSTAR Extended Life Test (ELT). The Labview-based software controls all power supplies and monitors and records thruster and facility telemetry. The engine is shut down in the event of any specified out-of-bounds condition (e.g. tank pressure or discharge voltage). Beam current and mass flow rates are auto-controlled by the DACS system to set values. The PC-based system is located remotely from the vacuum tank, away from the power supplies, etc., for operator safety and comfort.

Xenon propellant is supplied from a high-purity feed system copied from the NSTAR ELT test facility. Three UNIT UFM-1661 meters monitor flow rates with total uncertainties of 2.5% of the full-scale of 10 sccm for cathode flows and 100 sccm for the main flow. All propellant line connections where line internal pressures are less than atmospheric are welded or under vacuum to preclude cathode contamination from fitting leaks. The flow system has integral ports for calibration, pump-out, and nitrogen purges. Flow rates were calibrated with a NIST-traceable system before testing.

### C. Test Plan

The NEXIS wear test setup and plan was governed by the objectives of the test. The first goal of the test was to establish test conditions that provide reasonable assurance of obtaining representative results for final flight conditions and hardware, i.e. those necessary for the Herakles thruster development [REF] in support of proposed Prometheus missions. After test conditions are chosen, the performance of the thruster at those conditions must be characterized over the length of the test. At the conclusion of the test, inspection and analysis are used to measure the wear rates of the known wear phenomena, identify unknown wear-related issues or wear phenomena, and identify thruster design issues related to wear, life, or performance degradation (if observed). The final goal is to demonstrate adequate thruster design maturity for the project to proceed to the next development step toward flight hardware. The NEXIS DM has already taken an important step in that path with the conclusion of vibration testing.

Selection of the nominal operating point for the wear test was based on system-level requirements for the Herakles thruster [REF] dictated by proposed Prometheus missions. Although the NEXIS thruster was originally designed for operation at a specific impulse (Isp) of 7500 sec, the Herakles nominal Isp of 7000 sec was selected for the wear test. The Herakles discharge propellant utilization design point of 92% was also used, and the beam current was chosen to match the average beam current density of the Herakles design. In addition to the nominal design point, several alternate operating points were selected for periodic performance measurements. The Prometheus project requirements call for  $\pm 2\%$  throttling in power and in thrust for peak-power tracking and trajectory variability, respectively. Together with the nominal condition these requirements added eight additional operating points to the test plan. The thruster was also characterized at the nominal NRA design point of 7500 sec and at a lower Isp of 6000 sec that was desirable from a Prometheus mission perspective for high-thrust operations.

Performance testing of the engine and optics was performed at regularly scheduled intervals. At the nominal wear test condition, discharge chamber performance curves (i.e. discharge losses vs. discharge propellant utilization efficiency) were obtained during the test at the nominal discharge voltage, and at the beginning and end of the test at off-nominal discharge voltages. Optics performance data (i.e. perveance and electron backstreaming limits and screen transparency) and neutralizer plume mode margin were also investigated. At the two off-nominal Isp conditions both engine and optics performance data were acquired; at the eight Herakles off-nominal points only performance data were taken.

Ion optics performance was measured using standard procedures. Perveance measurements were made by holding the beam current and accelerator grid voltage constant while varying the screen grid voltage and recording the accelerator grid current. The discharge current was adjusted in this case to maintain constant beam current. The perveance limit was defined as the point at which the rate-of-change of accelerator grid current was 0.02 mA/V. Electron backstreaming (EBS) onset was determined by reducing the magnitude of the accelerator grid voltage at constant discharge current and monitoring the beam current, a 1% change in which defined the EBS limit. The screen grid transparency to ions was measured by biasing the screen grid negative of the cathode by twenty-five volts and recording the bias current. The ratio of the screen power supply current to the total current (i.e. bias current plus screen supply current) yielded the transparency.

A full suite of pre-test inspections and characterizations was performed in order to facilitate accomplishment of the test objectives. The ion optics dimensions were measured and the optics assembly gap and alignment were measured. Grid gap uniformity was better than 5% across the entire span of the 57-cm-dia. beam area. The discharge cathode condition was documented, including cathode and keeper orifice plate diameters and profilometry. Magnetic field mapping and plasma spray adhesion tests on the discharge chamber surfaces were performed. The thruster was completely photodocumented at the component and assembly levels. The total mass of the wear test article was 29.1 kg.

### III. Results and Discussion

The NEXIS DM1a thruster was operated for a total of 2020 hours during the wear test. During this period it processed 47.3 kg of xenon and experienced neither significant changes nor adverse trends in performance. The carbon backscatter rate from thruster-induced facility sputtering was  $7 \mu\text{m}/\text{hr}$  measured near the thruster exit plane. The facility cryopumps were turned off three times during the test, once because frequent pressure spikes were observed which suggested xenon buildup on cryosail surfaces, and twice for repair of facility support equipment (i.e. liquid nitrogen valve and water manifold). During these times the tank pressure reached  $\sim 1$  Torr.

#### A. Thruster Run Time Parameters

Controlled parameters for the nominal wear test condition are summarized in Table 1. These values were typically regulated to within  $\pm 0.5\%$ . Active closed-loop control of the beam current was achieved through variation of the discharge current to achieve the target value. Data for the dependent parameters and engine performance displayed in the following figures are shown as real data acquired by the DACS at twenty-minute intervals; there is no averaging or removal of any data points in the figures. Data points which were acquired during recycle events or performance testing are evident in the figures. Indicator lines have been drawn on the figures to designate performance test and cryopump regeneration times to facilitate interpretation.

**Table 1. Wear Test Controlled Parameters.**

Vs	4760 V
Va	-500 V
Jb	4.08 A
Jk	1.0 A
Jnk	3.0 A
mdotm	54.7
mdotc	6.1
mdotn	4.6

Discharge current and voltage over the course of the wear test are shown in Fig. 3. Engine operating conditions were changed slightly during the first 50 hours of the test to achieve the desired operating conditions as the thruster and facility came into thermal equilibrium. Overall, an increase in discharge voltage of approximately 0.3 V was observed during the test. Discharge current varied to maintain constant beam current in the face of small variations in discharge voltage, but as will be shown later the discharge losses did not increase after the first 500 hours of the test. Diurnal temperature variations in the facility induced minor fluctuations in uncontrolled

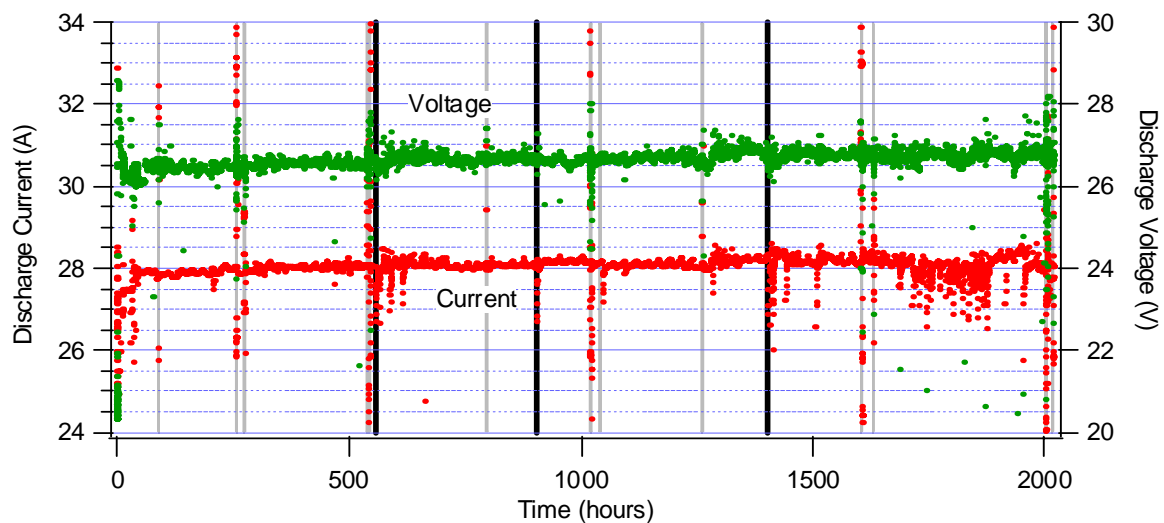


**Figure 3. Discharge Current and Voltage. Dark bars represent cryopump regeneration events and grey bars represent when performance measurements occurred.**

parameters as is observed near the 1200 hour mark, for example. Relatively frequent thruster restarts are visible in the discharge current data near the end of the test that resulted from electrical noise penetration into the DACS system which was corrected before the end of the test.

Performance of the neutralizer, namely the keeper and coupling voltage, is shown in Fig. 4. The coupling voltage was steady throughout the test at -16 V, slightly higher than nominal for other extended tests because of larger distance between the thruster and neutralizer to reduce interaction of its plume with stray thruster magnetic fields. Neutralizer keeper voltage decreased by nearly a volt over the course of the test. A step change in the keeper voltage occurred at 1870 hours when the neutralizer flow rate was increased by 0.4 sccm (neutralizer keeper discharge noise was observed in the DACS system at this time, related to the previously mentioned thruster restarts).

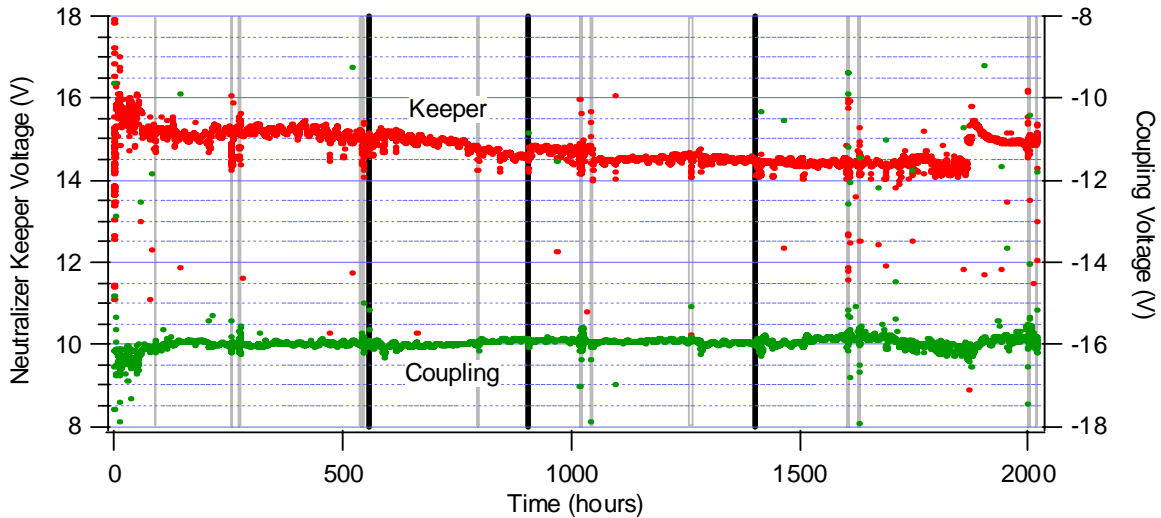


**Figure 4. Neutralizer Performance.** Dark bars represent cyropump regeneration events and grey bars represent when performance measurements occurred.

Total thruster power and tank pressure are shown in Fig. 5. Several hours to the better part of a day were required for the thruster and chamber to come into thermal equilibrium and this is reflected in tank pressure variations after thruster restarts. Pumping capacity of the cryosails in the bottom endbell was slightly reduced as the beam dump heated to operational temperature. Diurnal pressure variations are also observed. The nominal tank

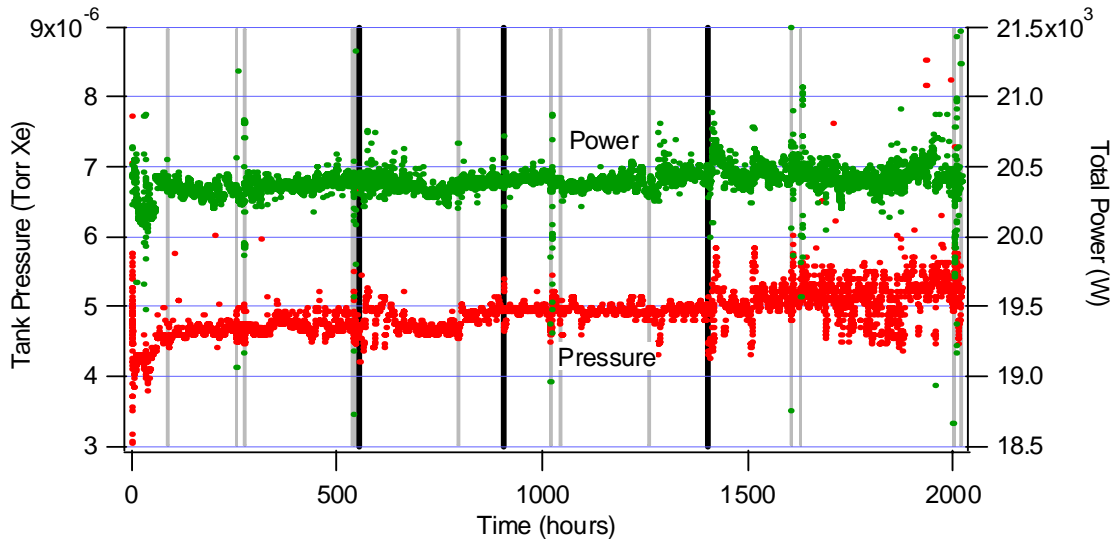


**Figure 5. Tank Pressure and Total Power.** Dark bars represent cyropump regeneration events and grey bars represent when performance measurements occurred.

pressure rose slightly during the test from  $4.6 \times 10^{-6}$  Torr to  $5.3 \times 10^{-6}$  Torr, likely related to hotter ambient temperatures coupled with carbon deposition on cryosail surfaces. Total thruster power was relatively stable at the 20.4 kW level.

Accelerator grid current as a function of time is shown in Fig. 6. Increases in current observed at about the 500 hour mark prompted a test for field emission which was observed as a current between the screen and accelerator grids of 200  $\mu$ A at the nominal wear test voltages with the thruster plasma discharges off. When plotted in the standard Fowler-Nordheim format it was verified that the current was field emission. There was no effect of xenon flow rate or thruster temperature on the levels of the observed vacuum current between the grids. Accelerator grid current of the operational thruster during the course of the test varied with time as seen in the figure. Large step changes in current levels were observed at the same times as some of the performance tests, i.e. at 1046, 1261, and 1605 hrs, as well as a very large change at 1953 hrs. Field emission currents were measured with the thruster off at several times during the test and the values obtained at the nominal wear test voltages are plotted in Fig. 6 also. The levels of vacuum field emission that were measured did not account for the difference in operational accelerator grid that were observed, e.g. at 1415 hrs the field emission current was 15 mA but the accelerator grid current was approximately 50 mA greater than the baseline value of 40 mA at the beginning of the wear test. The reason for the difference is not presently understood. At times when the accelerator grid current was near the baseline value there was no detectable field emission current at the nominal grid voltages (e.g. 1050 hrs).

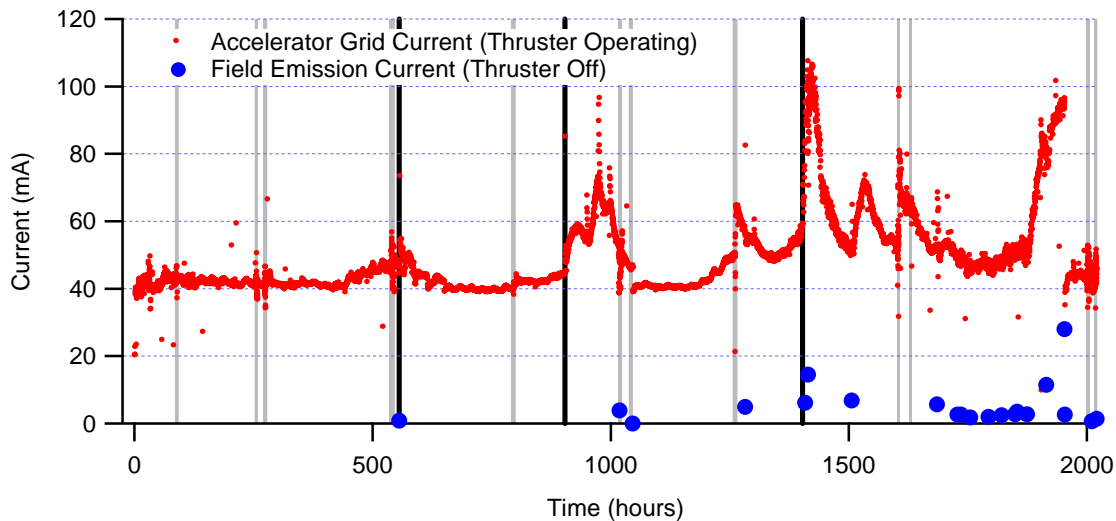


**Figure 6. Accelerator Grid Current. Dark bars represent cyropump regeneration events and grey bars represent when performance measurements occurred.**

Additional understanding of the field emission behavior with time can be achieved when inspecting the current-voltage curves as displayed in Fig. 7. It can be seen that the threshold electric field for field emission is varying with time, likely the result of evolution of field emitter sites with time. Surface morphology is altered by ion bombardment but also by localized heating and blowoff of the field emitter tips via emission current because of their relatively high resistance. It is also known that the controlled charge transfer of 1 mC during recycle events removes field emitter sites by arc conditioning. Thresholds of 1.8 to 2.1 kV/mm were observed when field emission current was present at the nominal 2.2 kV/mm. Threshold were greater than 2.2 kV/mm, of course, at times when field emission current was not present at the nominal voltages. These results indicate that if the NEXIS ion optics had been operated at more moderate electric field strengths then the field emission currents would not have been observed.

Before the test had concluded and the post-test inspection performed, it was postulated that excessive charge transfer during recycle events had roughened the accelerator grid surface, thus creating field emitter sites [REF]. Although this hypothesis was supported at the time with the test data available, post-test inspection of the accelerator grid revealed a complete lack of physical evidence for such events as will be discussed later. The field emission currents observed in Figs. 6 and 7 were not caused by excessive charge transfer during recycle events.

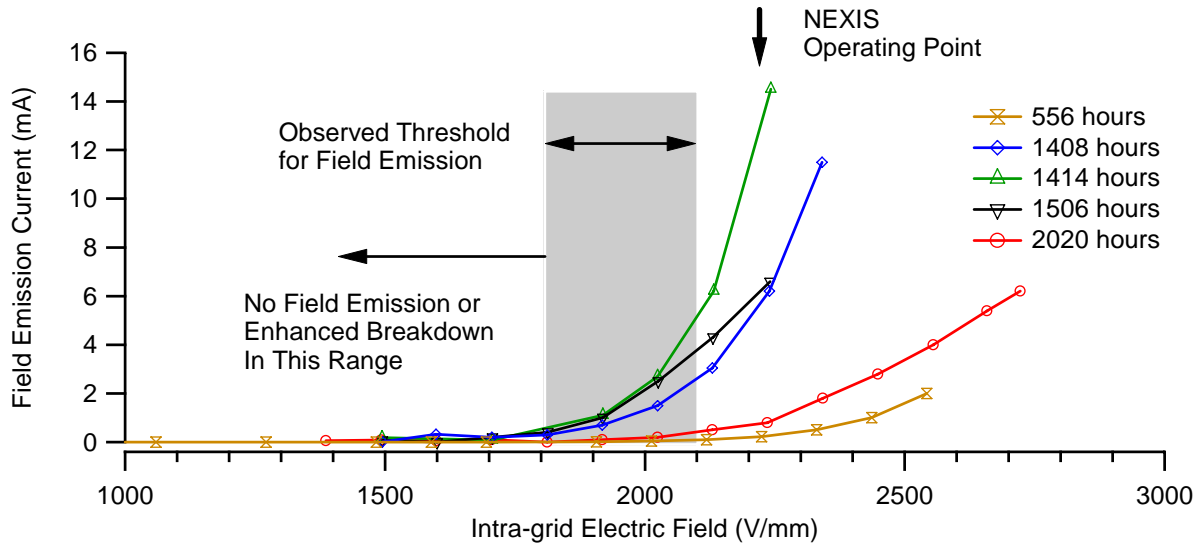


**Figure 7. Field Emission Threshold.**

### B. Engine and Optics Performance

Overall engine performance of the NEXIS engine is shown in Fig. 8. Although diurnal variations are present as well as Isp and efficiency decreases associated with neutralizer flow increase near the end of the test, engine performance was stable during the test. No significant changes nor long-term trends are apparent in the data. This is expected because of the stability of the run-time parameters already discussed.

Discharge losses, an important performance parameter and indicator of cathode health, are shown in Fig. 9. Losses were initially 177 eV/ion, increasing to 181 eV/ion over the first 200 hours, to 184 eV/ion by 500 hours, then were stable with slight variations from 183 to 185 eV/ion for the duration of the test. Full discharge performance curves, shown in Fig. 10, confirm that the discharge performance was stable after 500 hours. The discharge loss increases in the first 500 hours are directly related to internal discharge cathode plasma potential increases that have been measured in the NEXIS laboratory model discharge cathode [REF AIAA 2004-3430]. The internal plasma potential increases early in life as the cathode insert surface conditions and evolves, which reduces the primary energy of electrons exiting to the thruster discharge chamber. Discharge modeling [REF JPC05 Herakles] shows

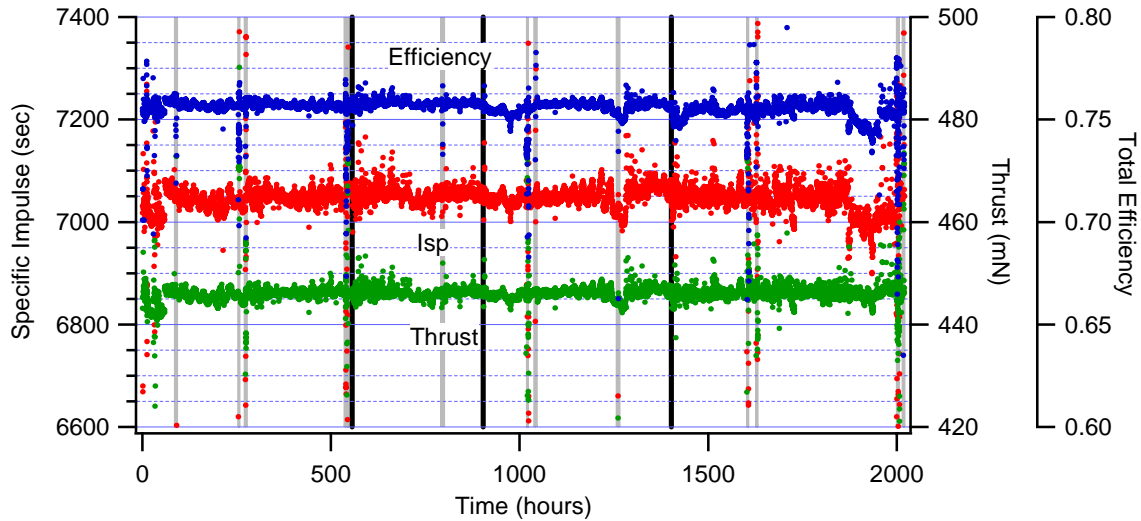


**Figure 8. Engine Overall Performance. Dark bars represent cyropump regeneration events and grey bars represent when performance measurements occurred.**

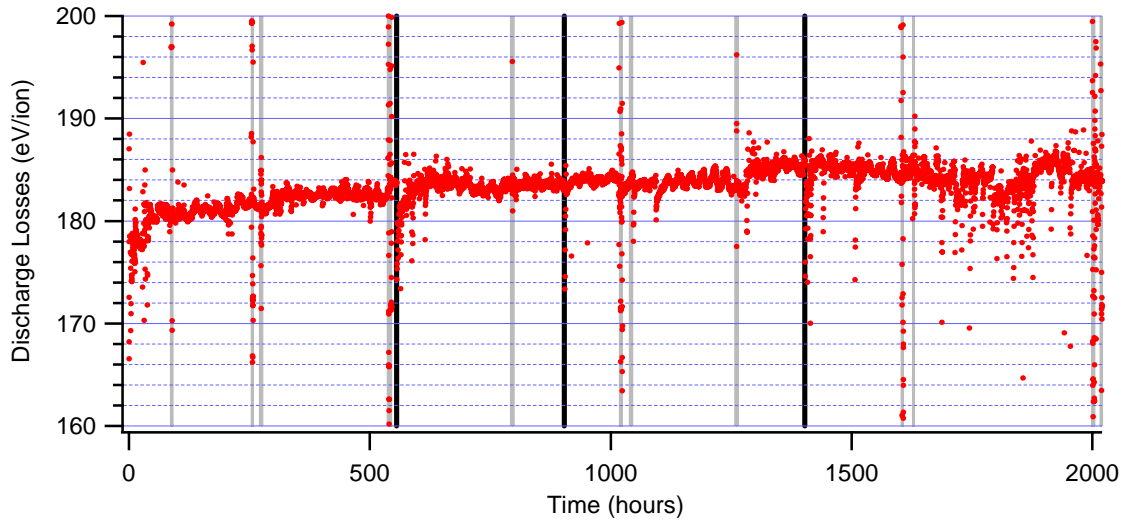


**Figure 9. Discharge Losses.** Dark bars represent cryopump regeneration events and grey bars represent when performance measurements occurred.

that the measured 0.7-V cathode plasma potential increase fully accounts for the observed change in discharge performance shown in Figs. 9 and 10.

Optics performance measured at 6000, 7000, and 7500 sec, shown in Figs. 11-13, was largely unchanged over the course of the test. No detectable changes in screen grid ion transparency (Fig. 11) were measured. Some scatter is observed in the perveance limit data at the nominal 7000-sec condition which is related to changes in field-emission currents during perveance testing. There appears to be a slight decrease in the perveance limit at 6000 sec (Fig. 12), but this increase in perveance margin is similar to the data scatter in the 7000 sec data. EBS limits (Fig. 13) were also steady over the course of the test, although a laboratory circuit limited collection of EBS data in the first half of the test.

Neutralizer performance, shown in Fig. 14, was stable near the flow rates used in the wear test and showed no change in plume mode margin. Large increases in coupling voltage, however, were observed at low flow rates near the end of the test. It is not clear what caused these changes, although they may be related to backspattered carbon deposition on the neutralizer keeper which had degraded the keeper-to-ground electrical isolation by the end of the test.

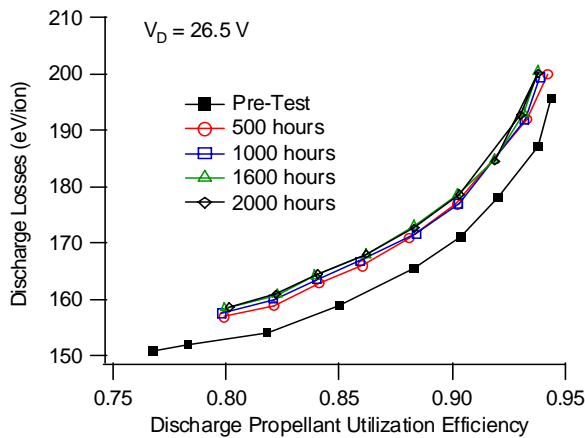


**Figure 10. Discharge Chamber Performance Curves.**

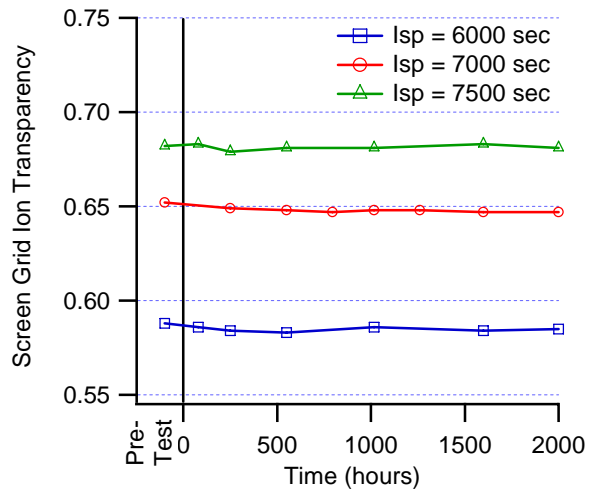


**Figure 11. Screen Grid Transparency.**

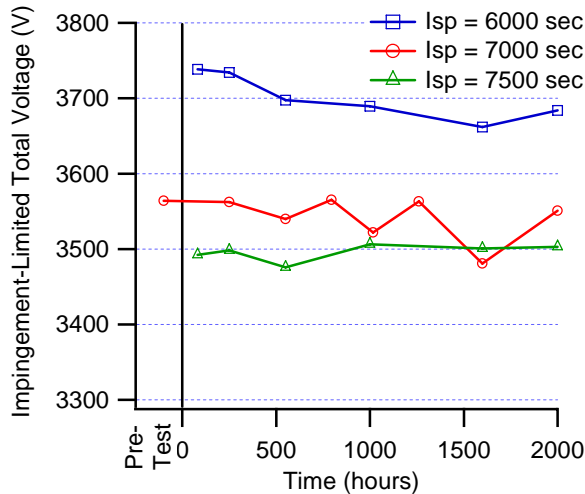


Figure 12. Perveance Limit.

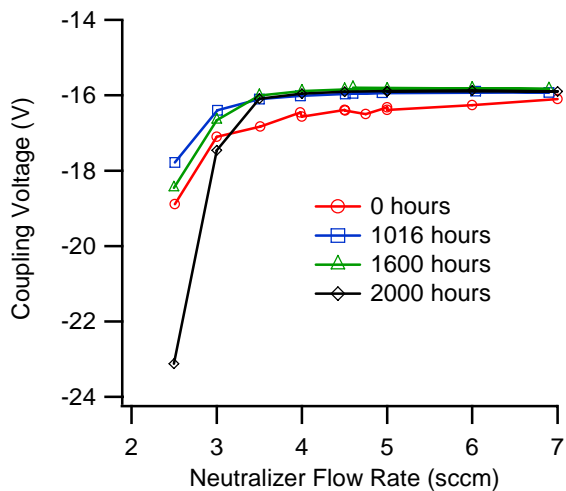


Figure 14. Neutralizer Performance.

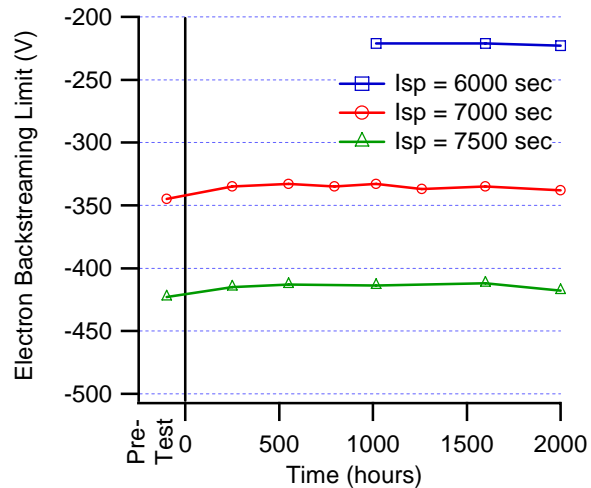


Figure 13. Electron Backstreaming.

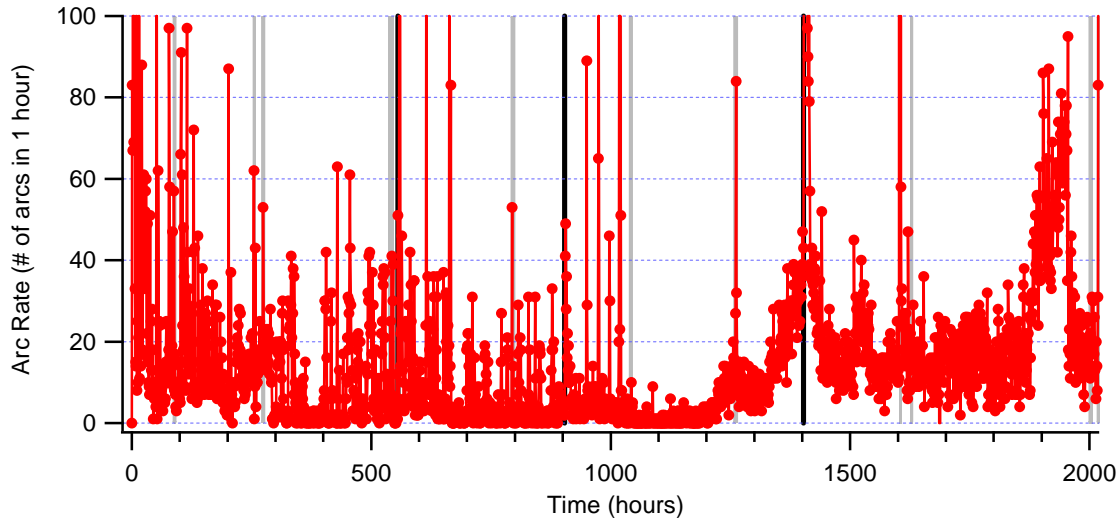
Engine performance at the 6000, 7000, and 7500 sec operating points is compared at various times throughout the test in Table 2. Following the trend of stability throughout the test for the nominal wear test condition, variations of only a few to several tenths of a percent are present in the performance data for the off-nominal Isp test conditions. As would be expected, data for the eight alternate Herakles throttling test conditions (i.e.  $\pm 2\%$  in thrust and power), not shown here, were also very stable during the course of the test.

### C. Post Test Inspection and Analysis

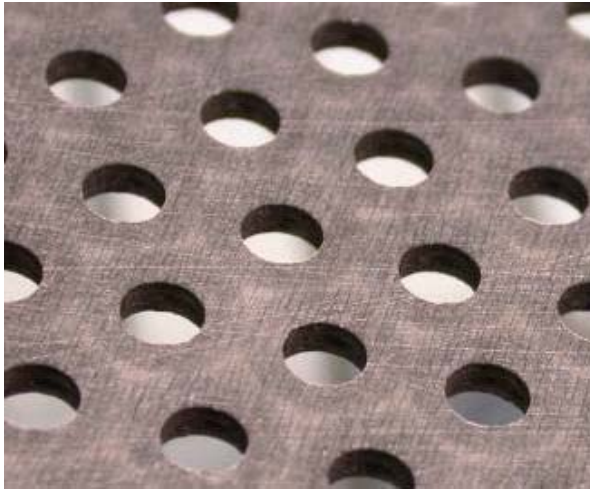
Of primary interest during the post-test disassembly and inspection of the thruster was the identification of the source of field emission current observed during the test and also the relatively high recycle rate, shown in Fig. 15. Recycle rate trends varied throughout the test, initially having “bursts” of recycles interspersed between quiet periods, then an extended period with low recycle rates of

Table 2. Comparison of Engine Performance Over Time for Three Main Test Conditions.

	Time (hours)	Total Power (kW)	Discharge Prop. Eff.	Discharge Losses (eV/ion)	Isp (sec)	Total Efficiency	Thrust (mN)
Nominal Wear Test Point	250	20.4	0.918	181.9	7023	0.757	446.0
	550	20.4	0.920	183.0	7038	0.756	446.0
	795	20.4	0.920	184.9	7030	0.758	446.3
	1016	20.5	0.920	184.3	7036	0.756	446.3
	1600	20.4	0.920	184.5	7021	0.755	446.0
	2000	20.4	0.920	184.4	7031	0.758	446.5
6000 sec	250	16.2	0.919	199.4	6044	0.745	406.2
	550	16.2	0.920	202.0	6034	0.742	406.6
	1016	16.2	0.917	201.0	6035	0.745	406.3
	1600	16.2	0.918	203.7	6037	0.744	407.3
	2000	16.2	0.919	203.5	6043	0.745	407.1
7500 sec	250	22.8	0.919	172.0	7517	0.762	471.6
	550	23.0	0.918	172.0	7535	0.756	472.0
	1016	23.0	0.916	172.0	7531	0.759	472.9
	1600	23.3	0.913	171.6	7502	0.750	473.4
	2000	23.1	0.911	172.0	7504	0.754	475.6



**Figure 15. Engine Recycle Rate. Rate is uncorrected for recycles occurring during performance testing and operator-induced diagnostic testing. Dark bars represent cyropump regeneration events and grey bars represent when performance measurements occurred.**



**Figure 16. Post-Test Inspection Photograph of Upstream Surface of Accelerator Grid. Note pristine, un-arc'd condition of surface.**

0-3 per hour, and finally sustained recycling at rates of ~15/hr and occasionally higher. The total number of recycles recorded during the test was 33,000. Recall, before conclusion of the test it had been postulated [JPC05 NEXIS] that excessive charge transfer to the accelerator grid during recycle events caused surface roughening and formation of field emitter sites. After removal and disassembly of the ion optics, the accelerator grid was thoroughly examined for physical evidence of arc damage. Arcing of material coupons at charge transfers of 5 mC is readily visible, and at 10 mC difficult to miss with the unaided eye [REF Dan HV arcing]. Inspection revealed that the upstream side of the accelerator grid was in pristine condition, however, as shown in Fig. 16. There was a complete lack of physical evidence for arc damage or obvious locations for field emission on the accelerator grid surface. Inspection of the downstream surface of the screen grid similarly had no physical evidence of arc damage, but did show localized discoloration on the edges of many apertures

which is attributed to heating by field-emission electrons accelerated through the intra-grid electric field.

Inspection of the thruster body after removal of the plasma screen revealed that the insulation on the wire harness had suffered significant decomposition. This was most evident near the discharge cathode as seen in Fig. 17, where the outer Teflon sleeving has remained intact but the insulation surrounding the electrical conductor has been almost completely removed. Wire insulation degradation including liquid decomposition products was observed up to 50 cm outside of the thruster plasma screen. Thruster design and assembly documents specified Teflon-coated wire sheathed in Teflon sleeving for electrical harness, but it was evident that non-Teflon-insulated wire had been inadvertently used. Analysis of intact insulation revealed that the insulation was PVC-based, known to decompose at temperatures well below the 240 °C measured during thruster performance testing. Heavy discoloration on the thruster external anode surface was observed near the wire location, especially on the magnet cusp locations. Corresponding discoloration was observed on the nearby locations of the plasma screen, especially along the magnetic field cusp line. None of these surfaces showed evidence of arcing or pitting.

The physical evidence strongly supports the presence of plasma discharges, not simply high-voltage arcs, between the anode and plasma screen in the rear portion of the thruster. The three elements required for electrical

breakdown were present: electrons from the ambient plasma which were able to penetrate the small mesh area in the plasma screen as observed before the wear test, a source of neutral gas (i.e. decomposing wire insulation), and high voltage. Localization of the events to the magnetic cusp further indicates that they were plasma discharges. The frequent breakdowns were observed in the telemetry as the fast-acting beam supply switch caused the high-voltage-to-ground discharge to be interrupted. It is concluded from the inspection of the thruster and grids that the majority of the recycles observed during the wear test were caused by the wire insulation decomposition.

Prior to the disassembly and physical inspection, the grid assembly was inspected for grid gap and alignment. The grid gap was determined by measuring the distance between the upstream surfaces of the screen and accelerator grids and subtracting the measured thickness of the screen grid. Post-test gap measurements across the entire active grid area are shown in Fig. 18. Apart from a single outlier data point that was likely a measurement artifact, the uniform control of the gap within 5% was unchanged; the measured normalized grid gap was  $1.02 \pm 0.03$  before and after the wear test. Likewise, no measureable changes in grid alignment were detected. Laser profilometry of the accelerator grid surface has also been performed to characterize the grid erosion experienced during the test, and the final results will be used for further refinement and validation of grid life models [REF CEX3D] which have already shown excellent predictive capability [REF JPC05 CBIO].

No problems were observed in the discharge cathode assembly when it was disassembled and inspected. The cathode heater heat shielding were intact and showed no damage and the cathode orifice plate showed the typical appearance of slight sputtering. No tungsten crystal formations nor foreign material depositions were observed in the cathode insert. The graphite keeper had loosely bound soot deposition on the outer diameter and in a thin ring surrounding the orifice as seen in Fig. 19. Apart from the latter deposition the keeper orifice plate was clean suggesting uniform ion bombardment. Laser profilometry of the plate indicated no detectable erosion (small machining grooves evident in the pre-test scans were still present in the post-test scans). This is in contrast to the significant keeper erosion observed in the 8000-hour NSTAR wear test [REF]. Keeper life modeling [REF Katz JPC05] in addition to fundamental plasma measurements of the cathode plasma discharge [Dan and Tina IEPC05] and the careful selection of cathode operating parameters suggest that the NEXIS cathode design will have a keeper life in excess of 100,000 hours.

#### D. Discussion of Field Emission Behavior

Post-test inspections of the thruster and ion optics have ruled out damage to the accelerator grid from excessive arc charge transfer as the cause of the observed electron field emission and frequent recycle rate. Although accelerator grid currents observed during recycle events were initially believed to be accel-grid-to-ground arcs [REF JPC05 NEXIS], it



**Figure 17. Post-Test Inspection Photograph of Wire Harness Near Discharge Cathode Assembly. Note decomposition of wire insulation inside the intact Teflon sleeving.**

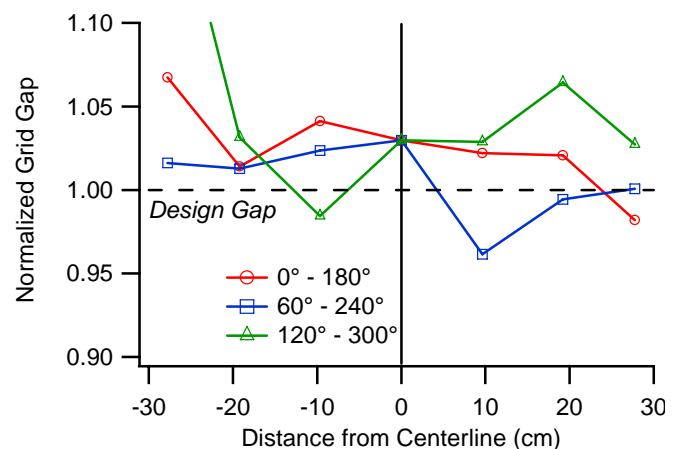


**Figure 18. Results of Post-Test Grid Gap Inspection.**



**Figure 19. Post-Test Photograph of Discharge Cathode Assembly Keeper Orifice Plate.**

was concluded that the current to the accelerator grid was instead ions pulled from the discharge chamber after the beam supply fast-acting switch terminated the plasma discharge in the rear of the thruster.

Electron field emission from the accelerator grid appears to have originated at the upstream edges of the accelerator grid apertures. Numerous indications of localized heating by collection of accelerated electrons are evident on the upstream edges of screen grid apertures across the grid surface. The sharp corners of the aperture edges enhance the local electric fields, promoting field emission from the negatively-biased accelerator grid and tending to focus collection of electrons on the positively-biased screen grid in those regions. Thruster test data also support accelerator grid aperture edges as the location of field emission current. The data in Figure 20, acquired during optics perveance testing at 1260 hours, show the effects of direct ion beam impingement on the nominal accelerator grid current. Before perveance testing the accelerator grid current had been steady at 50 mA. During perveance testing, as the screen voltage is decreased at constant beam current, direct impingement of accelerator grid surfaces occurred. After the perveance test and all nominal test conditions had been restored to their values prior to perveance testing (i.e. 2pm in the figure), the accelerator grid current was steady at the increased value of 65 mA. These same effects were observed at other times during the wear test. This is a direct indication of the evolution of field emitter sites at the accelerator grid apertures caused by ion bombardment. Such phenomena have also been demonstrated in testing of carbon-based gridlets [REF CSU IEPC].

The time dependence of the field emission current observed during the wear test (Fig. 6) is likely related to the competing effects of field emitter site evolution by ion bombardment and the documented “self-healing” of the surface by 1-mC arc charge transfer [REF DAN HV, CSU IEPC]. Optics performance testing, as well as the ion bombardment of the accelerator grid during the numerous recycle events cause by wire outgassing, evolved field emitter sites across the accelerator surface. Field emission was mostly likely at the aperture edges where the electric field was enhanced by the sharp edges. Field emitter sites were then removed by conditioning of the accelerator grid surface through 1-mC charge transfers. Net field emission from the accelerator grid likely increased as the evolution of field emitter sites dominated over their removal by conditioning. Net conditioning of field emitter surfaces has been demonstrated in gridlet testing [CSU IEPC] and was also observed at the 1950 hour mark of the wear test, where within a period of 2-3 hours there were very frequent conditioning arcs which caused the operational accelerator grid current to fall rapidly from a 95-mA peak to the beginning-of-test value of 40 mA. During this time period the vacuum field emission was occasionally measured and it was observed to fall from 30 mA to undetectable at the nominal wear test voltages.

Investigation of the voltage standoff of the carbon-carbon material used in the NEXIS grids was performed with small coupons in a ball-and-plate test where the threshold for field emission was arbitrarily defined as 1  $\mu$ A [REF Dan HV arc] in a specific region of the sample. It was determined from those tests that fields of 4 kV/mm could reliably be held off for non-apertured, undamaged materials. Introduction of apertures and of surface modification by arcing was found to reduce the threshold voltage for field emission. Evolution of field emitter sites over the much larger area of the NEXIS grids by ion bombardment could be expected to show larger currents at similar electric fields because of the greater number of field emitter sites. Gridlet experiments have demonstrated that the apertured carbon-carbon can be conditioned to hold off fields of up to 10 kV/mm with the application of several hundred conditioning arcs [REF CSU IEPC]. The physical area of the NEXIS ion optics is roughly fifty times larger than the gridlet area in those tests, suggesting some tens of thousands of conditioning arcs required to fully condition grids of the NEXIS size. The majority of the 33,000 recycles in the wear test occurred in the rear of the thruster instead of between the grids, and thus the grids were not able to be fully conditioned in the face of accelerator grid surface evolution by ion bombardment.

The results of the NEXIS wear test, combined

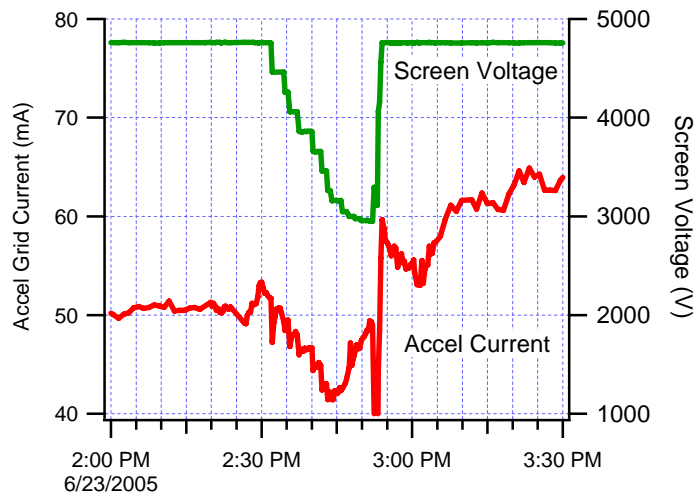


**Figure 20. Effect of Accelerator Grid Ion Beam Impingement on Field Emission Current. Direct ion bombardment causes evolution of field emitter sites.**

with the ball-and-plate materials tests and the gridlet tests, suggest that field emission behavior from carbon-based grids is complex interaction of the evolution of field emitter sites by ion bombardment, removal of those sites by conditioning of grid surfaces by controlled arc charge transfer, and that there may be an appreciable effect of grid surface area on the net behavior of grid surfaces. These phenomena should be characterized and well understood for future implementation of larger-sized carbon-based grids.

#### IV. Conclusion

The NEXIS Development Model thruster successfully completed a 2000-hour wear test intended to characterize thruster operation and wear phenomena at high-Isp, high-power operating points in support of the Prometheus project. Engine operation was stable throughout the test and showed no measurable performance degradation after initial conditioning of the discharge cathode insert. Discharge performance was steady after an initial 500-hour period in which cathode conditioning caused an increase of  $\sim 6$  eV/ion. Stability of discharge losses is essential for demonstrating the ability to meet challenging mission performance requirements for extremely long life times. Engine thrust, specific impulse, and efficiency reached the target values and remained steady. There were no significant measurable changes in ion optics performance. Thruster performance at off-nominal operating points followed this trend of stability for the duration of the test.

Relatively high recycle rates were observed during the test and were concluded to result from plasma discharges in the rear of the thruster between the anode and plasma screen, supported by neutral gas produced by wire insulation decomposition. The post-test condition of the accelerator grid surface was pristine, ruling out arc damage to that surface as the cause of observed field emission current between the screen and accelerator grids. Test data, post-test inspection, and the results of fundamental materials experiments indicate that ion bombardment of the accelerator grid during recycle events and optics performance testing evolved field emitter sites with time, causing the time-variable field emission. These effects were counteracted by self-cleaning of the grids through application of 1-mC conditioning arcs. The remaining issues from the test are then elimination of high-voltage breakdowns in the back of the thruster and control of ion bombardment of the accelerator grid surface.

The many successes of the NEXIS DM development, vibration test, and wear test are applicable to near-term NASA missions in addition to the targeted high-power, high-Isp Prometheus project goals. The design methodology was fully validated by test; discharge chamber and ion optics models agreed very well with measured performance. Engine performance was excellent, meeting all target requirements for NEP missions to the outer planets with performance stability during the 2000-hour wear test. Initial evaluations of component wear and performance suggest that the NEXIS DM thruster would perform to mission specifications for the required lifetime. Structural design models produced hardware which demonstrated the ability to survive vibration testing. Significant advances in grid manufacturing technology were achieved with a doubling of carbon-carbon grid size while improving grid gap and hole pattern control. Finally, the NEXIS design approach very rapidly matured hardware with significant infusion of new technologies, resulting in a final configuration that with few modifications could readily proceed to Engineering Model hardware.

#### Acknowledgments

The authors wish to acknowledge the significant contributions of John Beatty, Ryan Downey, John Anderson, Ray Swindlehurst, and Allison Owens to the work contained herein. We also thank Mike Patterson of the NASA Glenn Research Center for providing a NEXT neutralizer for the wear test. The research described in this paper was carried out by the Jet Propulsion Laboratory, California Institute of Technology, under a contract with the National Aeronautics and Space Administration in support of Project Prometheus.

#### References

1. S.R. Oleson, "Electric Propulsion Technology Development for the Jupiter Icy Moons Orbiter Project," AIAA 2004-5908, Space 2004 Conference and Exhibit, San Diego, CA, Sept. 2004.
2. T.M. Randolph and J.E. Polk, "An Overview of the Nuclear Electric Xenon Ion System (NEXIS) Activity," AIAA 2004-5909, Space 2004 Conference and Exhibit, San Diego, CA, Sept. 2004.
3. D.M. Goebel, J.E. Polk, and A. Sengupta, "Discharge Chamber Performance of the NEXIS Ion Thruster," AIAA 2004-3813, 40<sup>th</sup> Joint Propulsion Conference, Fort Lauderdale, FL, July 2004.

4. J.E. Polk, D.M. Goebel, J.S. Snyder, A.C. Schneider, and A. Sengupta, , “NEXIS Ion Engine Performance and Wear Test Results,” AIAA-2005-4393, to be presented at the 41<sup>st</sup> Joint Propulsion Conference, Tucson, AZ, July 2005.
5. J.R. Brophy, “NASA’s Deep Space 1 Ion Engine,” Review of Scientific Instruments, Vol. 73, No. 2, Feb. 2002, pps. 1071-1078.
6. J.R. Beattie, “XIPS Keeps Satellites on Track”, The Industrial Physicist, June 1998.
7. J.S. Beatty, J.S. Snyder, and W. Shih, “Manufacturing of 57cm Carbon-Carbon Composite Ion Optics for the NEXIS Ion Engine,” AIAA 2005-4411, to be presented at the 41<sup>st</sup> Joint Propulsion Conference, Tucson, AZ, July 2005.
8. J. Monheiser, J.E. Polk, and T.M. Randolph, “Conceptual Design of the Nuclear Electric Xenon Ion System,” AIAA 2004-3624, 40<sup>th</sup> Joint Propulsion Conference, Fort Lauderdale, FL, July 2004.
9. NEXIS Vibe JPC05.